

# Picosecond Time-Resolved Fluorescence Spectroscopy of (Z)-1-(2-Anthryl)-2-phenylethene and Its Model Compounds: Understanding the Photochemistry by Distinguishing between the *s*-cis and *s*-trans Rotamers

Takashi Karatsu,<sup>\*,†</sup> Hajime Itoh,<sup>†</sup> Atsuko Nishigaki,<sup>‡</sup> Keiji Fukui,<sup>†</sup> Akihide Kitamura,<sup>\*,†</sup> Shigeki Matsuo,<sup>§</sup> and Hiroaki Misawa<sup>§</sup>

Department of Materials Technology, Faculty of Engineering, and Center for Frontier Electronics and Photonics, Chiba University, 1–33 Yayoi-cho, Inage-ku, Chiba 263-8522, Japan, and Faculty of Engineering, The University of Tokushima, Minamijosanjima-cho, Tokushima 770-8506, Japan

Received: September 15, 1999; In Final Form: May 24, 2000

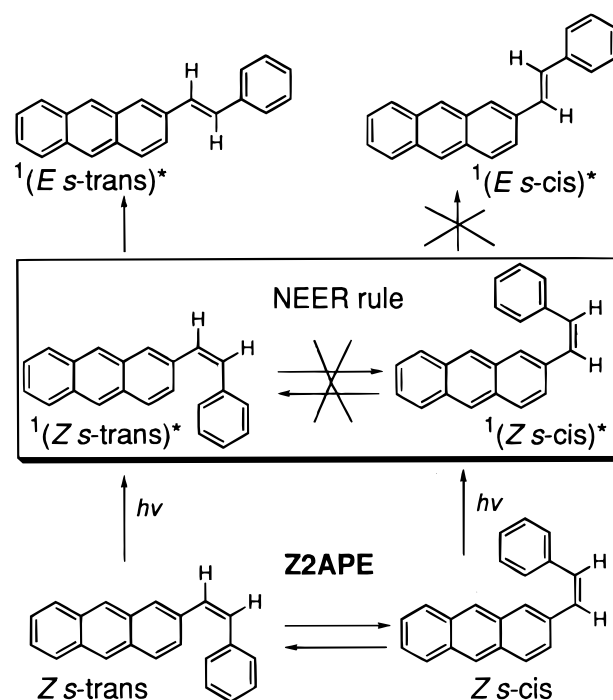
The photochemical reactions (*Z*–*E* isomerization and photocyclization) of the *s*-cis and *s*-trans rotamers of (Z)-1-(2-anthryl)-2-phenylethene (Z2APE) were investigated. The absorption, steady-state and picosecond time-resolved fluorescences, and transient absorption spectra were measured in order to achieve a better understanding of the rotamer photochemistry. The spectra were compared with those of the model compounds ((Z)-1-[2-(1-methylanthyryl)]-2-phenylethene: Z1Me2APE and (Z)-1-[2-(3-methylanthyryl)]-2-phenylethene: Z3Me2APE). It is confirmed that the *s*-trans rotamer undergoes only *Z*→*E* adiabatic isomerization and that the *s*-cis rotamer mainly photocyclizes to give the dihydrophenanthrene-type intermediate with a much faster rate constant ( $k_{\text{cyc}} = 2.3 \times 10^{10} \text{ s}^{-1}$ ). The reason Z2APE does not give an aromatized photocyclization product (1,2-naphtho[*a*]anthracene, NA) is that the return of the dihydrophenanthrene-type intermediate to the *Z* isomer is much faster than the oxidation to produce NA.

## Introduction

The compound 1-(2-anthryl)-2-phenylethene (2APE) has two rotational isomers with respect to the single bond that connects the anthryl group to the olefinic double bond. The *s*-trans- and *s*-cis-rotamers align their double bonds along the long and short axes of the anthryl moiety, respectively. The rotational isomerization of 2-anthrylethenes in the ground state and in the excited states is a subject of current interest.<sup>1–24</sup> Most of the studies have detailed the *E* isomer, because of its ease of preparation and its inactivity in the geometrical isomerization known as one-way *Z*→*E* isomerization.<sup>23–29</sup> This isomerization has been studied using steady-state fluorescence,<sup>1,2</sup> time-correlated single-photon counting (SPC),<sup>3–9</sup> time-gated fluorescence spectroscopy,<sup>10–13</sup> principal component analysis with self-modeling (PCA-SM),<sup>3,4,14–17</sup> and T–T absorption spectroscopy.<sup>18–21</sup> When compared with the extensive studies on the rotamers of the *E* isomers, only a few studies have been reported for the *Z* isomers.<sup>22–24</sup> In particular, the selective photochemistry of the two rotamers of (Z)-2APE (Z2APE) was elucidated by Saltiel's group using the PCA–SM technique.<sup>23,24</sup> They showed that in toluene (1) the NEER (nonequilibrium of excited rotamers) principle<sup>1,30,31</sup> holds for the singlet excited Z2APE, (2) that the <sup>1</sup>(*Z s*-trans)\* rotamer undergoes efficient adiabatic *Z*→*E* one-way isomerization, but that the <sup>1</sup>(*Z s*-cis)\* rotamer does not adiabatically isomerize to the *E* isomer (Scheme 1).

In our previous reports,<sup>18,19</sup> we characterized the *s*-trans and *s*-cis rotamers of E2APE by using their model compounds, in which methyl groups restrict their conformations as previously

## SCHEME 1



reported for the analogous naphthalene derivatives.<sup>15,32,33</sup> We attempted to characterize the *s*-trans and *s*-cis rotamers of Z2APE along the same lines by comparing their properties with those of the model compounds: (Z)-1-[2-(1-methylanthyryl)]-2-phenylethene (Z1Me2APE) and (Z)-1-[2-(3-methylanthyryl)]-2-phenylethene (Z3Me2APE). The study of the Z2APE rotamer and its analogues is particularly difficult, because one-way *Z*→*E*

\* To whom correspondence should be addressed, e-mail: karatsu@xtal.tf.chiba-u.ac.jp, FAX: +81-43-290-3039.

<sup>†</sup> Faculty of Engineering, Chiba University.

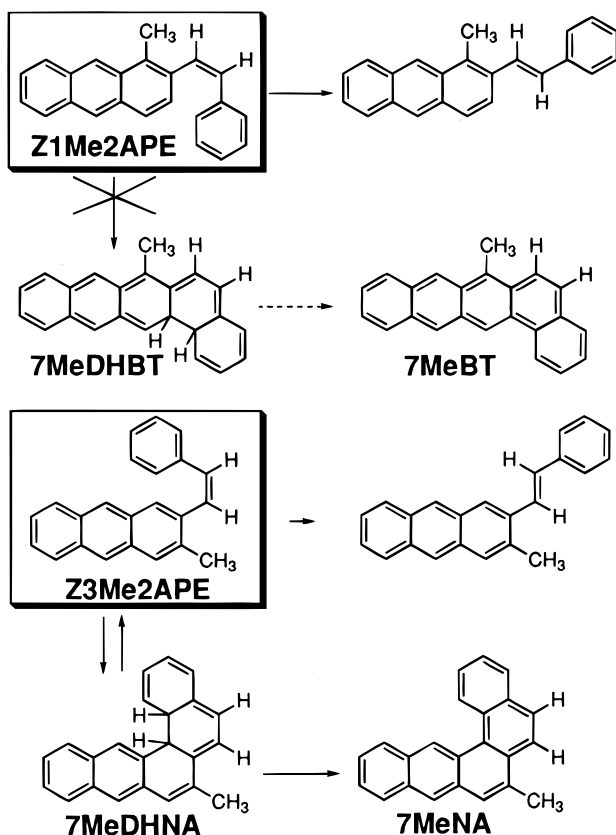
<sup>‡</sup> Center for Frontier Electronics and Photonics, Chiba University.

<sup>§</sup> The University of Tokushima.

geometrical isomerization efficiently takes place in  $S_1$ , and the fluorescence quantum yield of the *E* isomer is higher than that of the *Z* isomer.<sup>23,24</sup> This difficulty was overcome in Saltiel's study in which the characterization of the rotamers was based on steady-state fluorescence and photoisomerization data. We have now succeeded in understanding the behavior of the rotamers of Z2APE in the excited state using time-resolved spectroscopy. Our results on the reaction kinetics obtained by time-resolved spectroscopy are consistent with the conclusions of Saltiel et al.<sup>23,24</sup> complementing the results from the *s-trans* rotamer and providing new insight into the behavior of the *s-cis* rotamer. In addition, 2APE does not yield the photocyclization product whereas the *p*-methyl derivative, (*E*)-1-(2-anthryl)-2-(*p*-methylphenyl)ethene (EpMe2APE), yields the photocyclization product.<sup>34</sup> It has been argued that the isomerization cannot be exclusively  $Z \rightarrow E$  one-way.<sup>24,34</sup> However, we found that Z2APE gave a photocyclization product in the presence of oxidizing agents and the  $Z \rightarrow E$  isomerization should still seem one-way.

Conformer-specific photocyclization of arylenes has been reported by many groups. Therefore, we have also investigated the reaction from this point of view.<sup>34–36</sup> We find that the model compound Z3Me2APE yields 7-methyl-1,2-naphtho[*a*]anthracene (7MeNA) as well as the *E* isomer (E3Me2APE). However, as expected based on the free valence theory (Scheme 2),<sup>35,36</sup> Z1Me2APE gives only the *E* isomer (E1Me2APE) and does not produce 7-methylbenz[*a*]tetracene (MeBT).

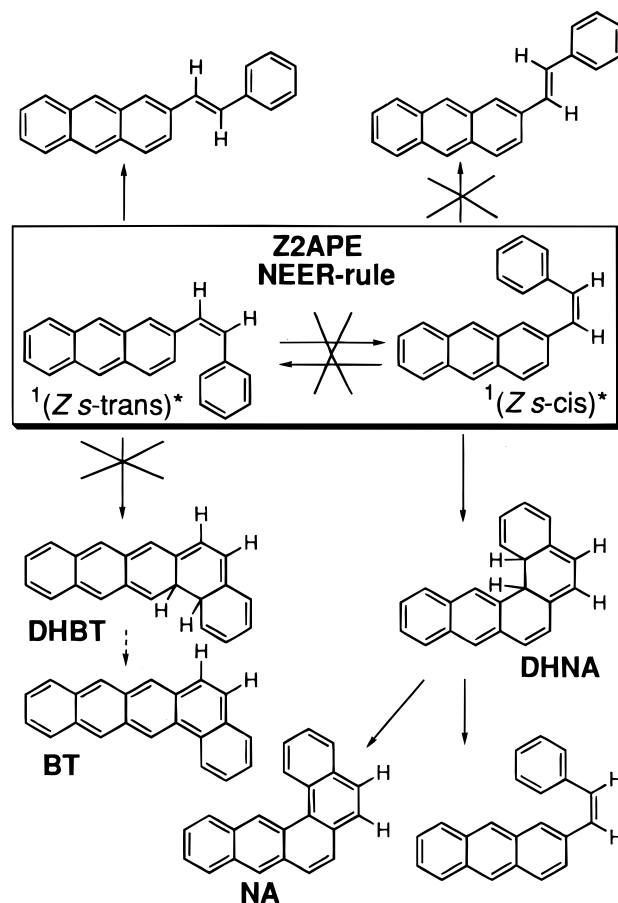
SCHEME 2



Z2APE yields a negligible amount of NA in the absence of iodine in air by the irradiation of 366 nm Hg arc light; however, we have determined that Z2APE gave a significant amount of NA in the presence of iodine in air, and this was due to the strong oxidizing ability of iodine. The absolute rate of oxidation by iodine determined in this study using a cryostat and pulsed

laser for excitation is about 40 times greater than that for oxygen. Therefore, air oxidation cannot compete with cycloreversion but iodine oxidation can, and the yield of NA increases in the presence of iodine (Scheme 3).

SCHEME 3



In addition to the fluorescence, the nanosecond time scale T–T absorption was examined for Z2APE to determine the behavior in the triplet state. At low temperature, the T–T absorption of the *E s-trans* isomer is observed just after laser pulse excitation, then the *E s-trans*  $\rightarrow$  *E s-cis* adiabatic rotational isomerization in  $T_1$  is observed as previously reported for the *E* isomer.<sup>19</sup> The spectral change indicates that the activation energy of the one-way  $Z \rightarrow E$  isomerization in  $T_1$  is smaller than that in  $S_1$  assuming that the preexponential factors of  $T_1$  and  $S_1$  are the same. The rate of intersystem crossing becomes higher than that of the  $Z \rightarrow E$  isomerization in  $S_1$  at the applied temperature (213 K).

Our results are complementary to the PCA-SM results<sup>23,24</sup> and supply information on the dynamics of the photochemistry of 2APE, including its photocyclization and one-way isomerization.

### Experimental Section

**Olefins and Other Chemicals.** 2APE, 1Me2APE, and 3Me2APE were prepared as reported previously.<sup>19,37</sup> Spectrograde benzene and methylcyclohexane (Dotite) were used without further purification. Guaranteed grade 2-methyltetrahydrofuran (Wako Chemicals) was purified by distillation over lithium aluminum hydride.

**Photochemistry and Product Analysis.** Stationary irradiation was performed with a 400-W high-pressure mercury lamp

using a UV-D36B glass filter (366 nm light, for direct excitation). Samples were prepared in benzene or methylcyclohexane and purged with argon or nitrogen, or degassed by three freeze-pump-thaw cycles. The *Z* and *E* isomers and cyclized products were analyzed by GC (Shimadzu GC-14A) with an OV-1 column (25 m) and HPLC systems (JASCO 880-PU) using a Senshu Pak Silica-1251-R (25 cm) column with a hexane-ethyl acetate (99:1) mixture. Absorption spectra were also measured using an HPLC-UV detector (Shimadzu SPD-M6A).

Photochemical products were identified by their mass spectra measured with a Shimadzu QP-2000 GC-MS spectrometer and by  $^1\text{H}$  NMR measured with a JEOL GSX-500. Quantitative analyses were performed by GC as mentioned above using chrysene as the internal standard.

Following irradiation at 355 nm from a Continuum Surelite I-10, the reaction rates of DHP for thermal reversion and reaction with oxygen or iodine were measured in methylcyclohexane with the use of a Hitachi U-3000 spectrophotometer using an Oxford DN1704 cryostat.

**Spectroscopy.** Absorption and emission spectra were measured with the use of a Hitachi U-3000 and of an F-4010 spectrometer, respectively. Fluorescence lifetimes in the nanosecond time range were measured with a Horiba NAES-550 single-photon counting spectrometer. The incident light was set at 360 nm and emission was collected through an L-40 or L-42 glass filter.

Fluorescence spectra and lifetimes in the picosecond time range were measured as described below. A Ti:sapphire laser (Spectra-Physics Tsunami, 1 mW, 150 fs fwhm, 4 MHz repetition) and a pulse selector (S-P model 3980) pumped by an  $\text{Ar}^+$  laser (S-P BeamLok model 2580) were used to obtain 380 nm incident light. Emission was focused by a lens (f30) on a monochromator (Oriel multispec 257, grating 150 g/mm, 2.6 nm resolution at a 100  $\mu\text{m}$  slit width) through an optical fiber (Oriel 77529). The detectors were a streak scope (Hamamatsu Photonics C4334-01) or a single photon counting detector (Hamamatsu Photonics MCP-PMT C2773) with a PC-module for time-correlated single photon counting (Becker & Hickl GmgH). Trigger signals were taken by a pin-photodiode through a delay unit (Hamamatsu Photonics C1097). Low-temperature experiments were performed with the cryostat.

T-T absorption spectra were measured with excitation at 355 nm (Continuum SL I-10, 6 ns fwhm, 20 mJ per pulse at 5 Hz repetition) using a detection system (Tokyo Instruments) composed of a multichannel diode array (Princeton IRY-512G: 18 ns gate width) with a SPEX 270M monochromator (resolution: 0.3 nm/channel). Decay profiles measured with a photomultiplier (Hamamatsu Photonics SR928) were analyzed by the Marquardt nonlinear least-squares fitting method. Low-temperature experiments were performed with the cryostat.

## Results and Discussion

**Absorption Spectra.** Figure 1 shows the absorption spectra of Z2APE, and its model compounds Z1Me2APE and Z3Me2APE in benzene for comparison. All compounds have broad absorption bands at 300 nm with bands with vibrational structure between 340 and 400 nm. The vibrational fine structure of Z2APE is very similar to that of Z1Me2APE but not at all like that of Z3Me2APE.

**Picosecond Time-Resolved Fluorescence Spectra.** The time-resolved fluorescence spectra were measured for the *Z* and *E* isomers of 2APE, 1Me2APE, and 3Me2APE in nitrogen-purged methylcyclohexane at various temperatures between 200 and 295 K. Figure 2 shows the fluorescence spectra of the *E* isomers

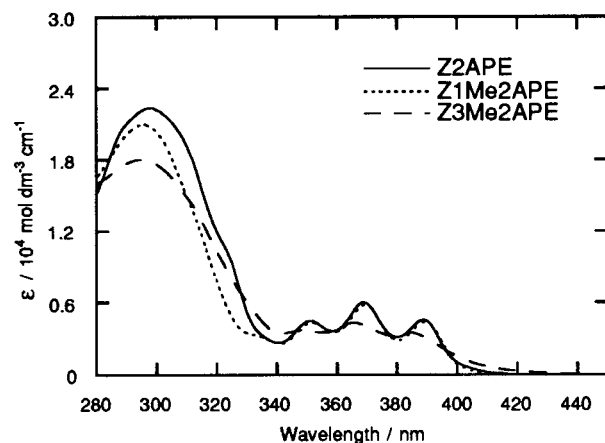


Figure 1. Absorption spectra of Z2APE, Z1Me2APE, and Z3Me2APE in benzene at ambient temperature.

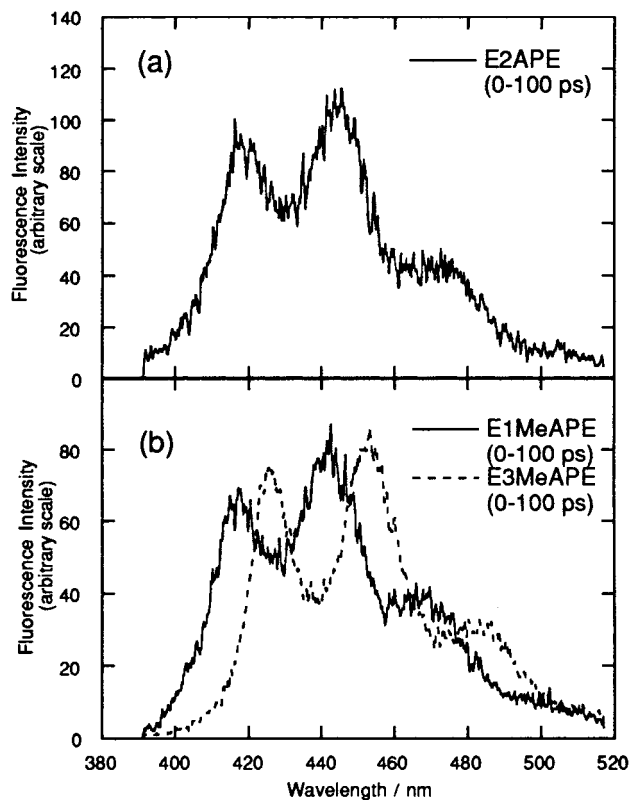
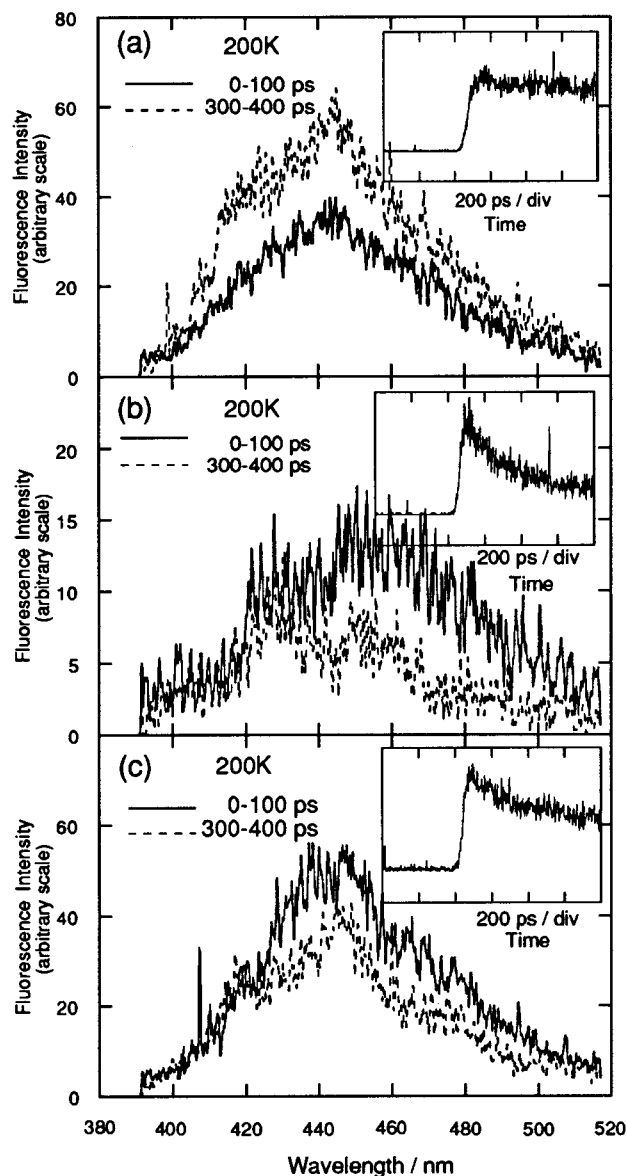


Figure 2. Time-resolved fluorescence spectra of (a) E2APE and (b) E1Me2APE (solid line) and E3Me2APE (dashed line) in nitrogen-purged methylcyclohexane at ambient temperature. The spectra were obtained by excitation at 380 nm and averaged between 0 and 100 ps after the laser pulses.

just after the laser pulse (average of CCD camera image through 0–100 ps). The spectra are essentially time-independent, at least up to 400 ps. The spectra of E2APE are known to be time-dependent, even obeying the NEER principle due to the different lifetimes of each rotamer;<sup>5,6</sup> however, no spectral change was observed in this short time scale. For E1Me2APE and E3Me2APE, the spectra are time-independent up to 400 ps, consistent with a single rotamer for each and are identical to the steady-state fluorescence spectra,<sup>2</sup> because the *E* isomer does not isomerize to the *Z* isomer and methyl substitution prevents rotational isomerization.

Figure 3a–c shows the fluorescence spectra with their typical time profile of the *Z* isomers of 2APE, 1Me2APE, and 3Me2APE, respectively, at 200 K. The spectra are time-



**Figure 3.** Time resolved fluorescence spectra (a, b, and c) and their time profiles (inset) of Z1Me2APE, Z3Me2APE, and Z2APE, respectively, at 200 K in nitrogen-purged methylcyclohexane. The spectra of solid and dashed lines were averaged on 0–100 ps, and 300–400 ps, respectively, after the laser pulses. The time profiles were averaged between 400 and 430 nm.

dependent up to 400 ps. Figure 3a shows the fluorescence spectra of Z1Me2APE; the spectra are assigned to the fluorescence of the *Z* isomer. At this temperature, the solution (in methylcyclohexane) still has fluidity;<sup>38</sup> however, we could not estimate the effective viscosity. The intensity between 0 and 100 ps is smaller than that between 300 and 400 ps, because the former includes the rise in the fluorescence in the excitation laser-pulse width. The spectrum at 300–400 ps contains a small amount of the fluorescence of the *E* isomer seen as a shoulder around 420 nm. The spectrum at 0–100 ps is broad and structureless as previously reported for Z2APE using the PCA–SM method.<sup>23,24</sup> Therefore, the decay profile (Figure 3a inset) is mainly due to the decay of the *Z* isomer and the lifetime is about 2 ns at 200 K. This value is slightly smaller than that in toluene,<sup>23</sup> but similar to that reported in the methylcyclohexane-3-methylpentane mixed solvent.<sup>29</sup> In Saltiel's reports, the *Z* *s*-trans excited state showed a quadratic concentration dependence of the fluorescence quenching of the adiabatically formed

*E* *s*-trans excited state;<sup>23,24</sup> however, such adiabatic *Z*→*E* isomerization through *S*<sub>1</sub> is prohibited at 200 K. For the spectra measured above 230 K, even at 0–100 ps, the contribution of the *E* isomer is significant, and a gradual increase in intensity of the *E* fluorescence was observed in the time scale of 100 ps. The observation of the *E* fluorescence just after laser excitation is unreasonable considering the lifetime of the *Z* isomer. Therefore, the emission comes from the re-excitation of the *E* isomer generated by adiabatic *Z*→*E* isomerization through *S*<sub>1</sub> (at higher temperature) or *T*<sub>1</sub> after the intersystem crossing (the rate of isomerization in *T*<sub>1</sub> is still high at 200 K, and it is very difficult to prevent this factor since we could not use a flow cell in a cryostat).

The time-resolved spectra and decay profile of Z3Me2APE at 200 K are shown in Figure 3b. The spectrum at 0–100 ps is assigned to the *Z* isomer, but the spectrum is mixed with the *E* isomer at 300–400 ps. This was also seen in the decay profile (Figure 3b inset). The decay consists of two components. The short-lived ( $\tau_s = 200$  ps) major component is the fluorescence of the *Z* isomer, and the minor other is the contribution of the *E* isomer as an impurity (purity of *Z* isomer is above 98%; however, the emission intensity of the *Z* isomer is very weak, therefore, such an influence becomes important). The reason fluorescence from the *Z* isomer of Z3Me2APE has such a shorter lifetime than that of Z1Me2APE is that the photocyclization reaction takes place at a much faster rate than the adiabatic *Z*→*E* isomerization in *S*<sub>1</sub>. Therefore, the decay rate mainly corresponds to the rate of the cyclization. This was also confirmed by the efficient formation of 7MeNA.

Figure 3c shows the behavior of Z2APE. Here, Z2APE has two rotamers, *s*-cis and *s*-trans, and the behavior of Z2APE is very similar to the mixed behavior of Z1Me2APE (model of the *Z* *s*-trans isomer) and Z3Me2APE (model of the *Z* *s*-cis isomer). At 200 K, the decay profile (Figure 3c inset) has two components with an equal contribution of the rotamers which have  $150 \pm 22$  ps and  $2 \pm 0.8$  ns lifetimes and almost a negligible contribution of the *E* isomer as seen in the time-resolved spectra (Figure 3c). This means that the decay profile and the spectra consist of the fluorescence of the short-lived *Z* *s*-cis rotamer and the long-lived *Z* *s*-trans rotamer.

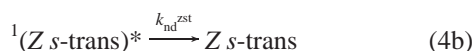
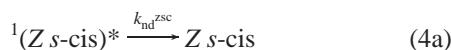
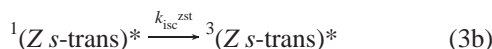
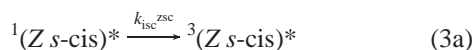
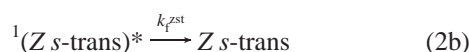
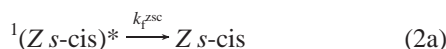
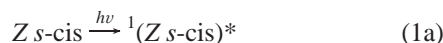
At temperatures higher than 230 K, the spectra and the decay profiles are very similar to those of the Z1Me2APE as described in the section on Z1Me2APE.

The spectra expected by the PCA–SM method for the *Z* isomer<sup>23,24</sup> are assigned to the *Z* *s*-trans isomer in toluene. In this report, the emission maximum of the spectrum is shifted by about 10 nm to a longer wavelength than that reported for the *Z* *s*-trans isomer by the PCA–SM method.<sup>24</sup> This is because our spectrum is assigned to the *Z* *s*-cis rotamer, and this 10 nm shift is for the longer wavelength of the *s*-cis rotamer compared to the *s*-trans rotamer. This is also seen in the rotamers of the *E* isomer.

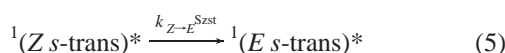
Fluorescence from the upper excited state (*S*<sub>2</sub>→*S*<sub>0</sub>) is reported for E2APE by PCA–SM method,<sup>16</sup> and this emission was also observed in methylcyclohexane. However, no further investigation has been done concerning the contribution of this excited state to the *Z*→*E* isomerization in this study.

The reaction mechanism is presented by the following equations. After excitation, each *Z* rotamer (equation numbers a and b and the superscripts *zsc* and *zst* of the rate constant correspond to the *s*-cis and *s*-trans rotamers, respectively) does the radiative (*f*; fluorescence) and nonradiative decays (*isc*, intersystem crossing; *nd*, nonradiative decay indicated by subscripts).



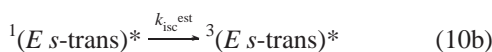
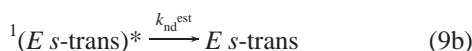
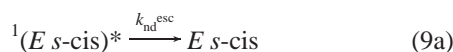
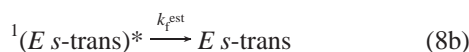


Saltiel et al. have shown that only the singlet excited state of the *Z s-trans* rotamer undergoes efficient *Z*→*E* adiabatic photoisomerization.<sup>23,24</sup> The absence of this process in the *Z s-cis* rotamer is probably due to its efficient cyclization to give DHNA (eq 6). Photocyclization of the *s-trans* isomer (eq 7) may be neglected as expected on the basis of MO calculations.<sup>35,36</sup>



For Z3Me2APE and Z1Me2APE, each olefin takes the *s-cis* and *s-trans* conformation, respectively, due to steric hindrance of the methyl groups; therefore, eq 6 is important only for Z3Me2APE.

The *E* isomers also undergo radiative and nonradiative decays (eqs 8–10). In these equations, the superscripts esc and est indicate the *E s-cis* and *s-trans* rotamers, respectively.



The lifetimes of the singlet excited state *Z* isomers are given by

$$\tau_S^{\text{zsc}} = 1/(k_f^{\text{zsc}} + k_{\text{isc}}^{\text{zsc}} + k_{\text{nd}}^{\text{zsc}} + k_{Z\rightarrow E}^{\text{Szsc}} + k_{\text{cyc}}^{\text{zsc}}) \quad (11)$$

$$\tau_S^{\text{zst}} = 1/(k_f^{\text{zst}} + k_{\text{isc}}^{\text{zst}} + k_{\text{nd}}^{\text{zst}} + k_{Z\rightarrow E}^{\text{Szst}}) \quad (12)$$

based on the results of obeying the NEER principle of the *Z* isomers as reported and no cyclization of the *Z s-trans* isomers. In Saltiel's report,  $k_{Z\rightarrow E}^{\text{Szsc}}$  is negligible and the temperature effect on  $k_{Z\rightarrow E}^{\text{Szst}}$  was extensively investigated in toluene.<sup>23</sup> From the results of the *s-trans* rotamer of Z2APE,  $k_{Z\rightarrow E}^{\text{Szst}} = 1.7 \times$

$10^8$  at 292 K is obtained, and also  $3.1 \times 10^6\ \text{s}^{-1}$  at 200 K is expected from their data. These values agree well with the results for Z1Me2APE (model of *s-trans*). However, in the cases of Z3Me2APE and Z2APE, the observed fluorescence has a much shorter decay component in the low-temperature range (around 200 K), and we believe that this is due to the contribution of fast photocyclization ( $k_{\text{cyc}}^{\text{zsc}}$ ) to the slow *Z*→*E* isomerization. To determine the Arrhenius parameters of photocyclization, the temperature dependence of the observed faster decay component was examined. However, this is extremely difficult because the increasing temperature causes increasing fluorescence of the *trans* isomer which disturbs the observation of the short lifetime component. Therefore, the parameters were roughly estimated for Z3Me2APE and Z2APE. For Z3Me2APE, the values of  $A = 6.8 \times 10^{10}\ \text{s}^{-1}$  and  $E_a = 8\ \text{kJ mol}^{-1}$  were roughly estimated using values of  $1310 \pm 71$  and  $886 \pm 63$  ps at 210 and 230 K, respectively. These correspond to  $k_{\text{cyc}}^{\text{zsc}} = 2.5 \times 10^9$  and  $5.7 \times 10^8\ \text{s}^{-1}$  at 290 and 200 K, respectively. For Z2APE, the observed short lifetime component is assigned to the *Z s-cis*, and the values of  $A = 4.9 \times 10^{12}\ \text{s}^{-1}$  and  $E_a = 13\ \text{kJ mol}^{-1}$  were also estimated roughly using the values of  $830 \pm 57$  and  $376 \pm 53$  ps at 190 and 210 K, respectively. The  $A$  factor for Z3Me2APE is slightly smaller than the typical values of the isomerization. This may have large experimental uncertainty because of experimental difficulty described above. These activation parameters correspond to  $k_{\text{cyc}}^{\text{zsc}} = 2.3 \times 10^{10}$  and  $2.0 \times 10^9\ \text{s}^{-1}$  at 290 and 200 K, respectively.

From the above kinetic treatment, it was found that the *Z s-cis* isomer mainly photocyclizes at 200 K and that the *Z*→*E* adiabatic isomerization competes with the cyclization at ambient temperature. However, for the *Z s-trans* isomer, the rate constant reflects the *Z*→*E* adiabatic isomerization because negligible cyclization occurred.

The photochemical paths of the *s-trans* isomer have been studied in detail by Saltiel et al.<sup>23,24</sup> Here, we roughly apply the kinetic data obtained above to Saltiel's precise kinetic analysis of the photochemical paths of Z2APE in toluene<sup>24</sup> that the cyclization is the main path for the *s-cis* isomer. The rate constant obtained for the cyclization is almost 2 orders of magnitude greater than the rate constants of the other paths such as fluorescence, intersystem crossing, and even adiabatic *Z*→*E* isomerization. Quantitative comparison of the rate constants from this study with those reported earlier<sup>23,24</sup> is hampered by the change in solvent; however, let us consider the rough estimation of the reaction paths. It makes clear the outline of the reaction mechanisms. In the case of 2APE, the quantum yields of fluorescence ( $\Phi_f$ ) of the *Z* and *E* isomers obtained in the steady state are reported to be 0.59 and 0.87, respectively,<sup>39</sup> in benzene at ambient temperature by us and 0.52 and 0.89, respectively,<sup>14,16,23</sup> in toluene by Saltiel et al. The difference in  $\Phi_f$  reported for the *Z* isomer was pointed out by the generation of the *E* isomer during the measurement since no flow cell was used in our earlier experiment.<sup>24</sup> It is reported by the PCA method<sup>24</sup> that the  $\Phi_f$  is composed of 25% ( $\Phi_f = 0.13$ ) fluorescence of the *Z* isomer and 75% ( $\Phi_f = 0.39$ ) fluorescence of the *E* isomer generated by the adiabatic *Z*→*E* isomerization. Therefore, at least 44% [(0.39/0.88) × 100] of the *Z* isomer adiabatically isomerizes to the *E* isomer in an adiabatic way. The intersystem crossing quantum yields ( $\Phi_{\text{isc}}$ ) of the *Z* and *E* isomers are reported to be 0.17 and 0.11, respectively.<sup>39</sup> Here, again, if one assumes that the observed triplet state was due to the isomerized *E* isomer, about 5% ( $0.11 \times 0.44 \times 100$ ) of the triplets was generated through the *E s-trans* singlet excited state after the singlet adiabatic *Z*→*E* isomerization. Therefore, almost

12% of the (0.17–0.05) triplets is generated through the intersystem crossing of the *Z* isomer, then triplet adiabatic *Z*→*E* isomerization occurred. In addition, the ratio production of the *E* *s*-trans rotamer through the singlet adiabatic *Z*→*E* isomerization and triplet adiabatic *Z*→*E* isomerization after intersystem crossing changes by the temperature, since  $k_{Z\rightarrow E^s}$  is dependent on temperature. In this assumption, we did not consider the change of reaction paths by changing energy levels of  $S_2$  and  $S_1$  state of the *E* *s*-trans isomer by temperature.

Values of 67% [ $k_{Z\rightarrow E^s}/(k_{Z\rightarrow E^s} + k_{isc} + k_f)$ ], 9% [ $k_{isc}/(k_{Z\rightarrow E^s} + k_{isc} + k_f)$ ] and 24% [ $k_f/(k_{Z\rightarrow E^s} + k_{isc} + k_f)$ ] were then expected at ambient temperature using the rate constants  $k_{Z\rightarrow E^s} = 1.7 \times 10^8 \text{ s}^{-1}$ ,  $k_{isc} = 2.4 \times 10^7 \text{ s}^{-1}$ , and  $k_f = 6.0 \times 10^7 \text{ s}^{-1}$  reported for the *s*-trans Z2APE in toluene.<sup>23</sup> These fit reasonably well to the values, 64% [(44/69) × 100], 17% [(12/69) × 100], and 19% [(13/69) × 100] obtained above for the *Z*→*E* isomerization, intersystem crossing, and fluorescence, respectively, for the *Z* *s*-trans isomer.

Finally, the missing 31% [ $100 - (44 + 12 + 13) = 1 - (\Phi_{Z\rightarrow E^{Zst}} + \Phi_{isc^{Zst}} + \Phi_{f^{Zst}})$ ], which we initially thought is a deactivation process at the twisted geometry, must be the efficiency of the photocyclization reaction as pointed out by Saltiel.<sup>23</sup> Considering the quantum efficiencies and kinetic values at 290 K mentioned above,  $k_{cyc}$  is exclusively faster than the other processes such as  $k_{Z\rightarrow E^s}$ ,  $k_{isc}$ , and  $k_f$ . Therefore, it is reasonably explained that the *s*-cis isomer solely undergoes photocyclization and that the *s*-trans isomer undergoes *Z*→*E* isomerization, intersystem crossing, and fluorescence. In addition, the large  $k_{cyc}$  value hampers estimating the other rate constants such as  $k_{isc}$  and  $k_f$ . The values of 31% and 69% then correspond to the population of the *s*-cis and *s*-trans isomers. These values show a slightly more equal population of each isomer than the reported value of around 80% of the *s*-trans isomer at ambient temperature ( $\Delta H = 3.9 \text{ kJ mol}^{-1}$ );<sup>23</sup> however, our rough estimation based on the experimental value is acceptable for understanding entire photochemical paths at this moment, but a more precise study of solvent effects should be done.

**Cyclization Reaction and Behavior of the Dehydrophenanthrene-Type Intermediates.** Figure 4 shows the change in the absorption spectra of Z3Me2APE, Z2APE, Z*p*Me2APE, and Z*m*Me2APE, before and after irradiation in argon-purged methylcyclohexane. For Z3Me2APE, the intermediate is stable enough to determine the reaction rate using a UV–visible spectrophotometer at temperatures between 200 K and room temperature with a cryostat. The sample solution was irradiated by 355 nm laser pulses (totally 50–100 pulses by 10 Hz), then the change followed by a spectrophotometer. The windows of the cryostat were covered by aluminum foil between each measurement. The plot of absorbance versus time was pseudo-first order. For Z2APE and Z*p*Me2APE, the spectral changes were very fast at room temperature; therefore, we have to observe these changes at temperatures below 250 K. Especially for Z*m*Me2APE, the spectral change due to the formation of an intermediate was very small even at low temperature. The decrease in the absorbance at the maximum with time is due to the thermal ring opening reaction of the dihydrophenanthrene-type intermediates to the *Z* isomers (eq 13)

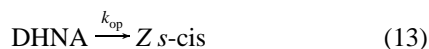
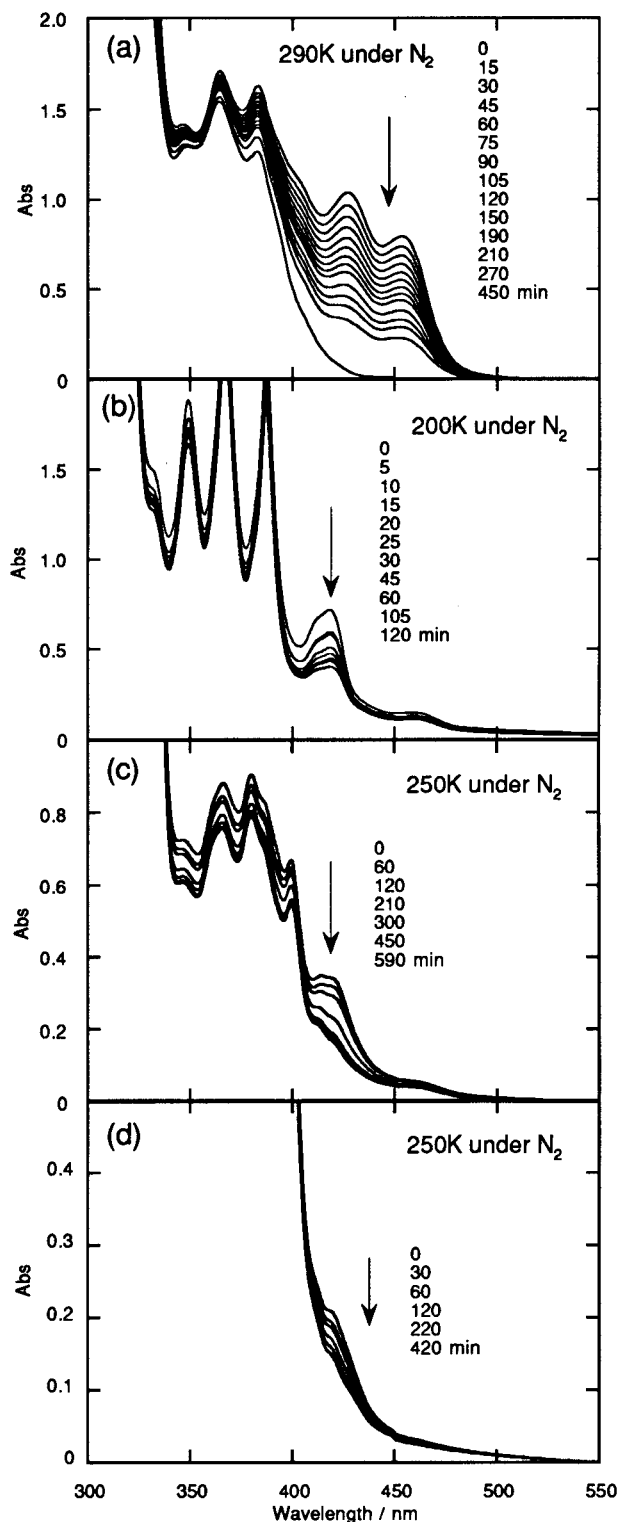


Figure 5 shows an Arrhenius plot of  $k_{opn}$  for the intermediates generated from Z3Me2APE, Z2APE, and (Z)-1-(1-anthryl)-2-phenylethene (Z1APE), which we reported,<sup>40</sup> for comparison. The preexponential factors (*A*) and the activation energies (*E<sub>a</sub>*)



**Figure 4.** Absorption spectral changes of Z3Me2APE (a), Z2APE (b), Z*p*Me2APE (c), and Z*m*Me2APE (d) by the 355 nm laser irradiation at 290, 200, 250, and 250 K, respectively, in methylcyclohexane.

are found to be  $A = 3.2 \times 10^2$ ,  $1.6 \times 10^2$ , and  $5.6 \times 10^6 \text{ s}^{-1}$ , and  $E_a = 4.3$ , 8.1 and  $14.9 \text{ kJ mol}^{-1}$ , for Z2APE, Z3Me2APE, and Z1APE, respectively. These *A* factors are very small for the unimolecular process; however, similar values are derived from the  $E_a$  values and the rate constant at the temperature reported.<sup>36</sup> The reason is not clear at this moment, and more work is apparently needed.

DHNA (14b, 14c-dihydro-1,2-naphth[*a*]anthracene) yields an aromatized product, NA (1,2-naphth[*a*]anthracene) by oxidation

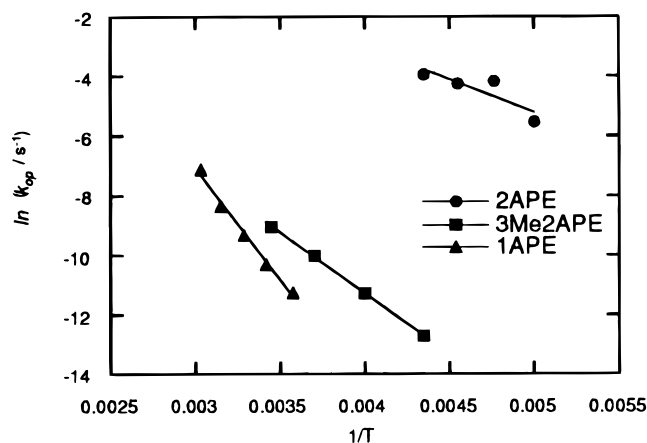


**Figure 5.** Arrhenius plots of the ring opening rate constant ( $k_{op}$ ) for DHP type intermediate of Z3Me2APE and Z2APE in methylcyclohexane determined in this study and Z1APE for comparison.

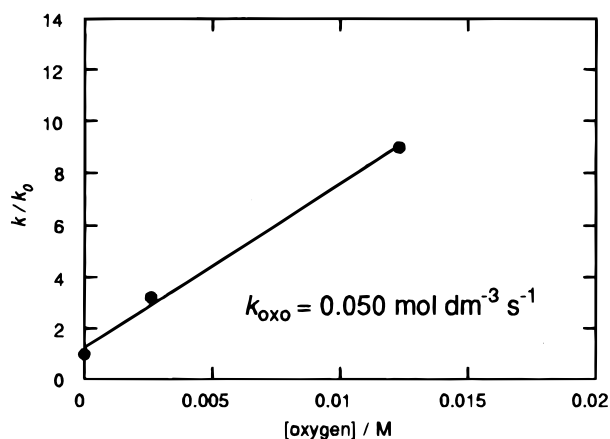


**Figure 6.** Oxidation rate constant for dihydrophenanthrene type intermediate of Z3Me2APE by oxygen ( $k_{oxo}$ ) in methylcyclohexane at ambient temperature.

in the presence of an oxidant such as molecular oxygen (eq 14) or iodine (eq 15). The spectral change was accelerated in the presence of the oxidants.



For Z3Me2APE, the oxidation rate constants of the DHP-type intermediates were determined by a Stern–Volmer-type plot of the rate versus the concentration of oxygen in solution (Figure 6). Only the intermediate generated from Z3Me2APE was relatively long-lived enough to determine the rate constants at ambient temperature. The sample solution containing oxygen or iodine was irradiated by 355 nm laser pulses (totally 50–100 pulses by 10 Hz), then the spectrum followed by a spectrophotometer at temperatures between 200 K and room temperature using a cryostat. The sample solution was irradiated by 355 nm laser pulses, and the change was followed by a spectrophotometer. The windows of the cryostat were covered by aluminum foil between each measurement. The plot of absorbance versus time was pseudo-first order. The absolute rate constants,  $k_{oxo}$ , was determined to be  $0.050 \text{ mol dm}^{-3} \text{ s}^{-1}$ . However, oxidation of dihydrophenanthrene by iodine is proposed to occur through a radical abstraction mechanism initiated by dissociation of iodine by light.<sup>41</sup> The rate of oxidation of DHNA is expected to depend on the concentration

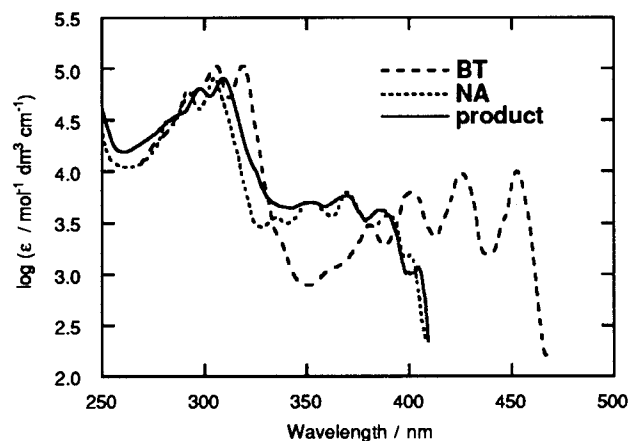


**Figure 7.** The absorption spectra of BT and NA in ethanol, reported in ref 41 and 42, respectively, and the absorption spectrum of product in benzene measured in this study.

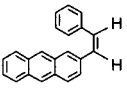
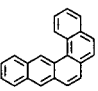
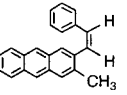
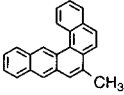
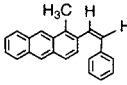
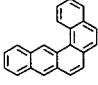
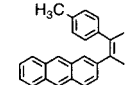
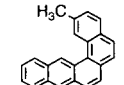
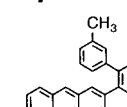
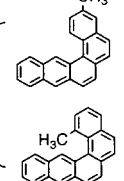
of iodine and light intensity. The rate was  $5.0 \times 10^{-4} \text{ s}^{-1}$  under room light when  $[\text{I}_2] = 1.9 \times 10^{-4} \text{ mol dm}^{-3}$  under these experimental conditions. This rate is about 6 times faster than the cycloreversion ( $7.8 \times 10^{-5} \text{ s}^{-1}$ ). The rate is expected to be greater under irradiation by a mercury lamp (366 nm) using a merry-go-round type photoreactor from which we obtained the photochemical product since the iodine atom is continuously generated by irradiation. We are doing more experiments to elucidate the oxidation mechanism by iodine.

Table 1 shows the products and yields by the irradiation of ZAPEs in air or in the presence of iodine in air. NA and 7MeNA were isolated and identified by the usual spectroscopic techniques, especially UV–vis absorption spectroscopy (Figure 7). Their spectra were compared with the spectra reported for NA<sup>42</sup> and benz[*a*]tetracene (BT).<sup>43</sup> In case of *Zp*Me2APE and *Zm*Me2APE, the products were identified only by GC–MS because of their low yields, and the yields were estimated based on the products (1MeNA, 2MeNA, and 3MeNA) having the same sensitivity to GC that 7MeNA has. The reason the yields for MeNA are different due to the methyl substitution at various positions is now under investigation using MO calculations. It is interesting that, in case of Z1Me2APE, NA having no methyl group was observed by GC–MS. The loss of the methyl or other groups by cyclization is sometimes observed as described in the literature.<sup>40</sup> In all cases, some oxygen-containing products were observed by GC–MS (the structures are expected to be like anthraquinone).

Conformer-specific photocyclizations of arylenes have been reported by several groups.<sup>35,36,40</sup> Especially, concerning *Zp*Me2APE, Laarhoven et al. reported the formation of 2MeNA in the presence of iodine.<sup>34</sup> This is in contrast to our initial report that no formation of NA occurred upon the irradiation of Z2APE.<sup>25–28</sup> This difference is discussed in relation to the one-way *Z*→*E* isomerization, and the formation of 2MeNA is due to the accumulation of the product during the reversible *Z*→*E* isomerization.<sup>24</sup> However, this study clarified why Z2APE did not give NA under the experimental conditions examined.

**T–T Absorption Spectra.** The adiabatic *Z*→*E* geometrical isomerization in the triplet excited state was examined by T–T absorption measurements. For the *E* isomers, our previous report showed that adiabatic *s*-trans to *s*-cis rotational isomerization occurs in the triplet excited state. For the *Z* isomer, the adiabatic *Z*→*E* isomerization in the singlet excited state is the main path; geometrical isomerization after intersystem crossing (eqs 16a and 16b) is not the dominant path, and only T–T absorption due to the *E* *s*-cis rotamer was observed at 290 K. However,

TABLE 1: Photocyclization Yields of (*Z*) 2-Anthrylethenes in the Presence and Absence of Iodine<sup>a</sup>

reactants	products	under air	in the presence of I <sub>2</sub> [I <sub>2</sub> ] = 1.0 × 10 <sup>-1</sup> mol dm <sup>-3</sup>
 <b>Z2APE</b>		2%	13%
 <b>Z3Me2APE</b>		19%	63%
 <b>Z1Me2APE</b>		trace	9%
 <b>ZpMe2APE</b>		trace	7%
 <b>ZmMe2APE</b>		none	trace
		none	trace

<sup>a</sup> Irradiated at 366 nm in methylcyclohexane (5.0 × 10<sup>-3</sup> mol dm<sup>-3</sup>) under air ([O<sub>2</sub>] = 2.6 × 10<sup>-3</sup> mol dm<sup>-3</sup>).

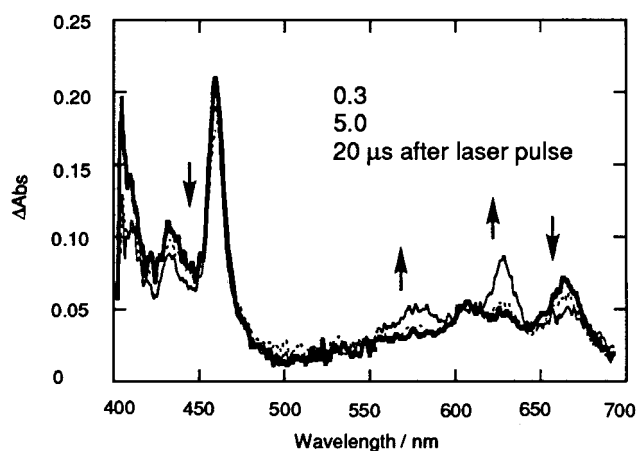
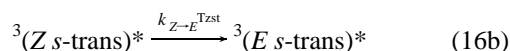
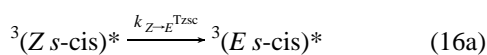


**Figure 8.** T-T absorption spectra of Z2APE in deaerated methylcyclohexane at 300 ns, 5 μs, and 20 μs after laser excitation at 213 K.

$k_{Z \rightarrow E^S}$  was suppressed and  $k_{isc}$  became the main path at low temperature. To estimate the population of each rotamer, the T-T absorption spectra were measured at low temperature (213 K) as shown in Figure 8. At 300 ns after the laser pulse, the spectrum is mainly due to the *E s-trans* rotamer, and a spectral change due to the *E s-trans* → *s-cis* adiabatic rotational isomerization was observed as seen in the rotational isomerization of the reported *E* isomer.<sup>18–20</sup> However, a spectral change due to the *Z* → *E* adiabatic isomerization as expressed in eqs 16a and 16b could not be observed because the isomerization is faster than the instrument resolution even at 213 K.



## Conclusions

In conclusion, we have determined the photochemistry of Z2APE by picosecond time-resolved fluorescence spectra by comparison of the spectra with those of two model compounds. The *s-trans* isomer is more stable in the ground state. Based on the fluorescence spectra, kinetic values, and analysis of the photoproducts, the *s-cis* rotamer solely photocyclizes in the singlet excited state, and the *s-trans* rotamer undergoes *Z* → *E* adiabatic isomerization. The cyclization process has a much smaller activation energy than that of the *Z* → *E* adiabatic isomerization. This conclusion essentially coincides with the earlier work done by Saltiel's group using principal component analysis. We have concluded that the efficient cyclization reaction prevents *Z* → *E* isomerization from the *s-cis* rotamer.

## References and Notes

- Mazzucato, U.; Momiccioli, F. *Chem. Rev.* **1991**, *91*, 1679–1719, and references therein.
- Fischer, G.; Fischer, E. *J. Phys. Chem.* **1981**, *85*, 2611–2613.
- Spalletti, A.; Bartocci, G.; Masetti, F.; Mazzucato, U.; Cruciani, G. *Chem. Phys.* **1992**, *160*, 131–144.
- Bartocci, G.; Mazzucato, U.; Spalletti, A. *Chem. Phys.* **1996**, *202*, 367–376.
- Ghiggino, K. P.; Skilton, P. F.; Fischer, E. *J. Am. Chem. Soc.* **1986**, *108*, 1146–1149.
- Wismontski-Knittel, T.; Das, P. K. *J. Phys. Chem.* **1984**, *88*, 1163–1168.
- Wismontski-Knittel, T.; Das, P. K. *J. Phys. Chem.* **1984**, *88*, 1168–1173.
- Arai, T.; Karatsu, T.; Sakuragi, H.; Tokumaru, K.; Tamai, N.; Yamazaki, I. *Chem. Phys. Lett.* **1989**, *158*, 429–434.
- Arai, T.; Karatsu, T.; Sakuragi, H.; Tokumaru, K.; Tamai, N.; Yamazaki, I. *J. Photochem. Photobiol. A: Chem.* **1992**, *65*, 41–51.
- Kang, T. J.; Etheridge, T.; Jarzeba, W.; Barbara, P. F. *J. Phys. Chem.* **1989**, *93*, 1876–1881.
- Brearley, A. M.; Strandjord, A. J. G.; Flom, S. R.; Barbara, P. F. *Chem. Phys. Lett.* **1985**, *113*, 43–48.
- Flom, S. R.; Nagarajan, V.; Barbara, P. F. *J. Phys. Chem.* **1986**, *90*, 2085–2092.



- (13) Brearley, A. M.; Flom, S. R.; Nagarajan, V.; Barbara, P. F. *J. Phys. Chem.* **1986**, *90*, 2092–2099.
- (14) Saltiel, J.; Zhang, Y.; Sears, D. F., Jr.; Choi, J.-O. *Res. Chem. Intermed.* **1995**, *21*, 899–921, and references therein.
- (15) Saltiel, J.; Eaker, D. W. *J. Am. Chem. Soc.* **1984**, *106*, 7624–7626.
- (16) Saltiel, J.; Zhang, Y.; Sears, D. F., Jr. *J. Phys. Chem.* **1997**, *101*, 7053–7060.
- (17) Saltiel, J.; Choi, J.-O.; Sears, D. F., Jr.; Eaker, D. W.; O'Shea, K. E.; Garcia, I. *J. Am. Chem. Soc.* **1996**, *118*, 7478–7485.
- (18) Karatsu, T.; Yoshikawa, N.; Kitamura, A.; Tokumaru, K. *Chem. Lett.* **1994**, 381–384.
- (19) Karatsu, T.; Itoh, H.; Yoshikawa, N.; Kitamura, A.; Tokumaru, K. *Bull. Chem. Soc. Jpn.* **1999**, *72*, 1837–1849.
- (20) Krongauz, V.; Castel, N.; Fischer, E. *J. Photochem.* **1987**, *39*, 285–300.
- (21) Laarhoven, W. H.; Cuppen, Th. J. H. M.; Castel, N.; Fischer, E. *J. Photochem. Photobiol. A: Chem.* **1989**, *49*, 137–141.
- (22) Saltiel, J.; Tarkalanov, N.; Sears, D. F., Jr. *J. Am. Chem. Soc.* **1995**, *117*, 5586–5587.
- (23) Saltiel, J.; Zhang, Y.; Sears, D. F., Jr. *J. Am. Chem. Soc.* **1997**, *119*, 11202–11210.
- (24) Saltiel, J.; Zhang, Y.; Sears, D. F., Jr. *J. Am. Chem. Soc.* **1996**, *118*, 2811–2817.
- (25) Arai, T.; Tokumaru, K. *Chem. Rev.* **1993**, *93*, 23–39, and references therein.
- (26) Karatsu, T.; Arai, T.; Sakuragi, H.; Tokumaru, K. *Chem. Phys. Lett.* **1985**, *115*, 9–15.
- (27) Arai, T.; Karatsu, T.; Misawa, H.; Kuriyama, Y.; Okamoto, H.; Hiresaki, T.; Furuuchi, H.; Zeng, H.; Sakuragi, H.; Tokumaru, K. *Pure Appl. Chem.* **1988**, *60*, 989–998.
- (28) Arai, T.; Tokumaru, K. *Bull. Chem. Soc. Jpn.* **1995**, *68*, 1065–1087.
- (29) Mazzucato, U.; Spalletti, A.; Bartocci, G. *Coord. Chem. Rev.* **1993**, *125*, 251–260, and references therein.
- (30) Jacobs, H. J.; Havinga, E. *Adv. Photochem.* **1979**, *11*, 305–373, and references therein.
- (31) Birks, J. B.; Bartocci, G.; Aloisi, G. G.; Dellonte, S.; Barigelletti, F. *Chem. Phys.* **1980**, *51*, 113–120.
- (32) Sun, Y.-P.; Sears, D. F., Jr.; Saltiel, J.; Mallory, F. B.; Mallory, C. W.; Buser, C. *J. Am. Chem. Soc.* **1988**, *110*, 6974–6984.
- (33) Saltiel, J.; Choi, J.-O.; Sears, D. F., Jr.; Eaker, D. W.; Mallory, F. B.; Mallory, C. W. *J. Phys. Chem.* **1994**, *98*, 13162–13170.
- (34) Laarhoven, W. H.; Cuppen, Th. J. H. M.; Nivard, R. J. F. *Tetrahedron* **1970**, 4865–4881.
- (35) Laarhoven, W. H. in *Organic Photochemistry*, Padwa, A., Ed.; Marcel Dekker: New York, 1989; Vol. 10, p. 163, and references cited therein.
- (36) Muszkat, K. A. *Top. Curr. Chem.* **1980**, *88*, 89–144, and references therein.
- (37) Karatsu, T.; Tsuchiya, M.; Arai, T.; Sakuragi, H.; Tokumaru, K. *Bull. Chem. Soc. Jpn.* **1994**, *67*, 3030–3039.
- (38) von Salis, G. A.; Labhart, H. *J. Phys. Chem.* **1968**, *72*, 752–754.
- (39) Arai, T.; Karatsu, T.; Tsuchiya, M.; Sakuragi, H.; Tokumaru, K. *Chem. Phys. Lett.* **1988**, *149*, 161–166.
- (40) Karatsu, T.; Kitamura, A.; Zeng, H.; Arai, T.; Sakuragi, H.; Tokumaru, K. *Bull. Chem. Soc. Jpn.* **1995**, *68*, 920–928.
- (41) Mallory, F. B.; Mallory, C. W. *Org. React.* **1984**, *30*, 1–456.
- (42) Clar, E.; Stewart, D. G. J. *J. Am. Chem. Soc.* **1952**, *74*, 6235–6238.
- (43) Clar, E.; Lombardi, L. *Ber.* **1932**, *65*, 1411–1420.